THE PLUMOSE BOULANGERITE FROM BOTTINO, APUAN ALPS, ITALY: CRYSTAL STRUCTURE, OD CHARACTER AND TWINNING

Gennaro VENTRUTI

Dipartimento di Scienze della Terra e Geoambientali, Università degli Studi di Bari, Via E. Orabona 4, I–70125 Bari, Italy

Francesca STASI

Via M. Mitolo 5, I–70124 Bari, Italy

Daniela PINTO[§] and Filippo VURRO

Dipartimento di Scienze della Terra e Geoambientali, Università degli Studi di Bari, Via E. Orabona 4, I–70125 Bari, Italy

Monica RENNA

Laboratorio Gemmologico, c/o Banco di Sicilia, Via A. Borrelli 20-22, I–90139 Palermo, Italy

Abstract

We deal with a single-crystal X-ray diffraction study of boulangerite from a plumose sample from the Bottino mine, Apuan Alps, Italy. Chemical composition of the analyzed sample is $Pb_{4.89}(Sb_{4.08}As_{0.04}Bi_{0.01})_{\Sigma 4.13}(S_{10.98}Se_{0.02})_{\Sigma 11.00}$. The crystal structure was investigated and evaluated in terms of the order–disorder (OD) theory. Boulangerite belongs to the subcategory Ia of OD structures composed of equivalent layers with symmetry $P(n)2_1m$. Two polytypes with maximum degree of order (MDO) are possible: MDO1 with space group $P12_1/a1$ and unit-cell parameters $a_1 \approx 21.61$, $b_1 \approx 23.54$, $c_1 \approx 8.05$ Å, $\beta_1 \approx 100.7$; MDO2 with space-group $P2_1/n11$ and unit-cell parameters $a_2 \approx 21.24$, $b_2 \approx 23.54$, $c_2 \approx 8.05$ Å, $\alpha_2 \approx 90$. Single-crystal X-ray diffraction patterns (Mo$K\alpha$, CCD detector) show strong reflections pointing to an orthorhombic substructure (the "family structure" in the OD terminology) and additional weaker reflections that correspond to the polytype MDO1. Frequent twinning with (100) as the twin plane was observed. The MDO1 structure was refined on a twinned crystal to $R = 0.062$ for 8495 reflections with $F_o > 4\sigma(F_o)$. Unit-cell parameters are a 21.554(4), b 23.454(4), c 8.079(2) Å, β 100.76(1) . The structure of boulangerite is composed of rods of SnS archetype six atomic layers thick and three pyramids wide. The central portion of these thick rods is characterized by ribbons of coordination pyramids of Pb and Sb atoms alternating along [001]; the marginal portions contain ribbons of coordination pyramids primarily occupied by Sb. In the refined structure, there are 18 independent cation sites: 10 are pure lead sites, six are pure antimony sites, two mixed positions split into two close sites occupied by Pb and Sb, respectively. On the basis of an OD interpretation, we assess the relationships between monoclinic and orthorhombic structures reported in the literature for boulangerite.

Keywords: plumose boulangerite, lead, antimony, sulfosalt, crystal structure, OD theory, twinning, Bottino, Italy.

Introduction

Boulangerite, $Pb_5Sb_4S_{11}$, is a rather common sulfosalt mineral occurring in lead and antimony ore deposits as fibrous masses, large felt-like masses or acicular aggregates. It was first discovered at Molières, France, by the French mining engineer Charles Louis Boulanger (1810–1849) (Boulanger 1835, Thaulow 1837). Owing to the extreme needle-like morphology of the crystals, boulangerite has recently attracted growing attention in material science as promising nanowire material for applications in selective absorption and catalysis (Krivovichev 2008) and in microelectronic devices (Heuer *et al*. 2004, Štrbac *et al*. 2010, Dittrich *et al*. 2007).

The crystals of boulangerite analyzed in this work were selected from large felt-like aggregates of Pb–Sb sulfosalts found at the Bottino mine, Apuan Alps, Italy; these aggregates are entered in the mineralogical collection of the University of Bari (Pelloux collection,

§   *E-mail address*: d.pinto@geomin.uniba.it

Museum Carlo L. Garavelli, Dipartimento di Scienze della Terra e Geoambientali) and labeled "plumosite". The term "plumosite", which was first introduced by Haidinger (1845) to identify sulfosalts exhibiting a hair-like habit, has been successively ascribed to a specific phase ($Pb_2Sb_2S_5$) related to but distinct from boulangerite (Berry & Thompson 1962, Born & Hellner 1960, Mozgova & Bortnikov 1980, Mozgova *et al*. 1983, Cook & Damian 1997). However, several investigators have raised doubts about the identity of "plumosite" and consider it as a plumose variety of boulangerite (Wang 1973, 1977, Smith & Hyde 1983, Mumme 1989, Moëlo *et al*. 2008). Samples of "plumosite" from Bottino were previously investigated by Garavelli (1957) and Stasi *et al*. (1998) by means of powder and single-crystal X-ray-diffraction data, respectively; both studies established the identity of the plumose material from this locality as boulangerite.

The aim of the present work is to provide a comprehensive crystal-structure study of boulangerite, which clarifies the links among the various structural models reported in the literature. The occurrence of orthorhombic and monoclinic phases, twinning phenomena, as well as the relationships between the 8 Å superstructure and the 4 Å subcell structure of boulangerite, have been interpreted through the application of the OD approach. In accordance with the indications given by the OD theory, careful refinement and description of the crystal structure of the monoclinic polytype MDO1 of the boulangerite OD-family were thus performed from high-quality single-crystal X-ray-diffraction data collected on a crystal of the plumose boulangerite from Bottino.

Background Information

The crystal structure of boulangerite has been extensively investigated by means of various X-ray photographs and powder techniques. Whereas the basic structural configuration of the mineral is known, a general confusion persists regarding its true structure model, degree of atomic order within the structure, as well as its relationship with "plumosite" (Breithaupt 1837) and falkmanite (Ramdohr & Odman 1940, Robinson 1948, Pruseth *et al*. 2001). Berry (1940) determined a monoclinic cell for boulangerite, *a* 21.6, *b* 23.5, *c* 8.1 Å, β 100.48°, space group $P2_1/a$, from single-crystal photographs of the material from the Gold Hunter mine, Mullan, Idaho. Born & Hellner (1960) found boulangerite to be orthorhombic, with cell parameters *a* 42.28, *b* 23.46, *c* 8.07 Å, and space group $Bb2_1m$; furthermore, they proposed a model for the orthorhombic subcell structure, lattice parameters *a* 21.14, *b* 23.46, *c* 4.03 Å (space group *Pbnm*), with a statistical distribution of Pb and Sb over three sites.

In their investigation of a monocrystal of boulangerite by means Weissenberg photographs, Dornberger-Schiff & Höhne (1962) observed distinct domains of different

symmetry. In particular, they noticed that the sharp spots, with *l* = 2n, exhibit orthorhombic symmetry, but the weak spots, with *l* = 2n + 1, show orthorhombic or monoclinic symmetry with respect to the particular crystal area irradiated; moreover, they found that additional non-space-group-related absences occur for the reflection with *l* = 2n, which were present only for *k* + *l* = 4n. On the basis of the peculiarities of the diffraction patterns, Dornberger-Schiff & Höhne (1962) argued that boulangerite belongs to the category of OD structures composed of equivalent layers. However, the OD groupoid symbol proposed by them did not explain the symmetry $Bb2_1m$ reported by Born & Hellner (1960). Using single-crystal X-ray-diffraction film-pack techniques, Mumme (1989) derived a monoclinic structural model [*a* 21.612(7), *b* 23.543(8), *c* 8.084(3) Å, β 100.71(2)°, space group $P2_1/a$] with an ordered distribution of cations. Orthorhombic subcell structures were described for synthetic crystals by Petrova *et al*. (1978a) and successively by Skowron & Brown (1990a). Bente & Anton (1995) inferred that ordered phases and OD phenomena occurring in natural samples involve Pb–Sb order, whereas disordered variants, described by a 4 Å submotif, show a statistical distribution of metals and have a higher symmetry. In a study of boulangerite single crystals from Bottino, Stasi *et al*. (1998) proposed a revised OD groupoid that proved to be more successful than that reported by Dornberger-Schiff & Höhne (1962) in describing all crystallographic and structural features of boulangerite.

Because of the key role of the OD approach in the refinement and description of the crystal structure of boulangerite performed herein, the next section will be devoted to an introduction of some basic concepts of the OD theory, as well as to the OD analysis of boulangerite.

An OD Description of Boulangerite

The OD theory applies to structures that are built up of one or more kinds of layers that can be stacked in two or more geometrically equivalent ways. This positional ambiguity between adjacent layers allows the existence of a series of both disordered and ordered sequences, the so-called OD family (Dornberger-Schiff 1956, 1964, 1966, Dornberger-Schiff & Fichtner 1972, Ďurovič 1997, Merlino 1997, 2009, Ferraris *et al*. 2008). An OD groupoid symbol characterizes the symmetry properties of all members of the OD family. This notation consists of two lines of symmetry operators, called partial operations (POs) in the OD terminology, as they are not necessarily valid for the whole crystal structure. The first line of the OD groupoid symbol gives the symmetry operations that bring each single layer into itself (λ operations). The second line gives the set of symmetry operations relating adjacent layers (σ operations). According to Stasi *et al*. (1998), the structure of boulangerite can be described as consisting of OD

layers of one kind with symmetry defined by the layer group $P(n)2_1m$ (hereafter the parentheses indicate the direction of missing periodicity) and crystallographic parameters referring to the monoclinic cell determined by Mumme (1989), $a_0 = (a \sin\beta)/2$ 10.618, b 23.543 and c 8.084 Å (Fig. 1). The set of σ operations compatible with this OD-layer group has been derived from the basic compilation of OD-groupoid families (Dornberger-Schiff & Fichtner 1972) through a permutation of axes. The resulting OD groupoid family symbol for boulangerite is:

$$P \quad (n) \quad 2_1 \quad m$$
$$\{(2_2) \quad n_{\frac{1}{2},2} \quad 2_{-\frac{1}{2}}\}$$

In the case of boulangerite, we deal with the subcategory Ia of OD structures, namely OD structures with both λ and σ POs that show layer-reversing (ρ type) and layer-non-reversing (τ type) character, and at least one interlayer r operation has reverse continuation (Ferraris *et al.* 2008). For this subcategory, the number (Z) of distinct positions of layer n + 1 with respect to the layer n is calculated from the so-called NFZ relation, $Z = N/F$, with:

N = 2 (E, [--m]), the subgroup of the non-reversing λ–τ operations;

F = 1 (E), the subgroup of the λ–τ operations that present continuation, *i.e.*, are valid for a pair of adjacent layers.

Therefore Z is equal to 2 for the present case. In fact, it is simply the combined action of the set of σ opera-
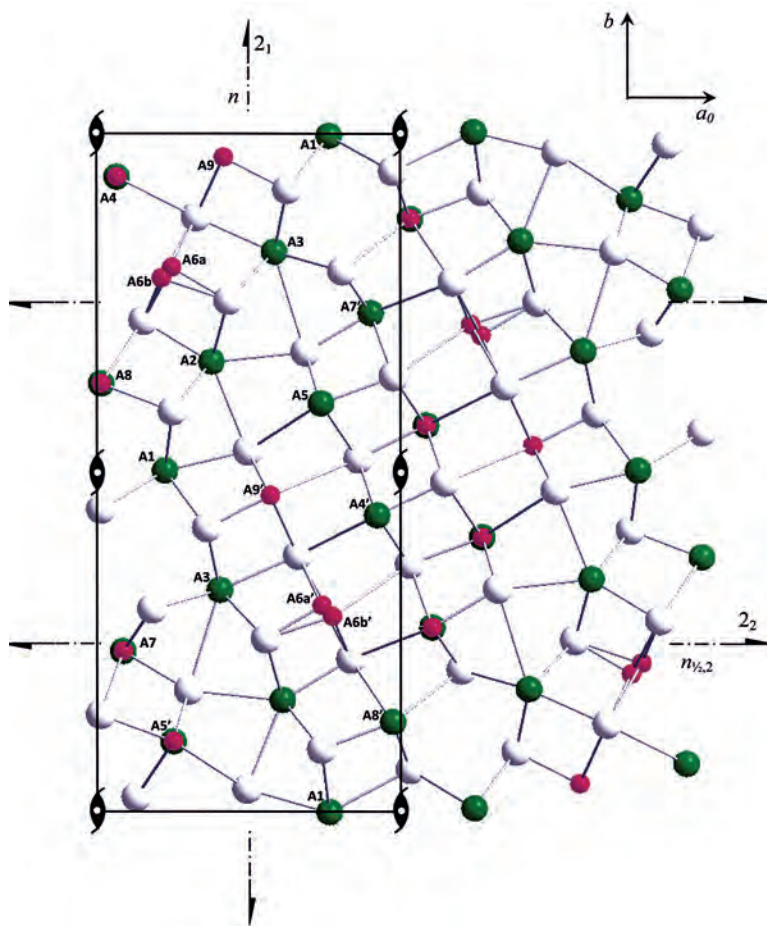

FIG. 1. A pair of adjacent equivalent OD layers seen along **b**. λ–PO and σ–PO are drawn. Site labels and unit cell of the equivalent layer are outlined. Spheres in order of decreasing size represent: S atoms (white), Pb atoms (green), and Sb atoms (pink).

tions with the symmetry plane normal to $\mathbf{c}$ in the OD layer that gives rise to two distinct positions of the layer $n + 1$ with respect to the layer n. Adjacent layers can be related through operations $[--n_{1/2,2}--]$ (and through $[--2_{-1/2}--]$ also), as well as through $[--n_{-1/2,2}--]$ (and through $[--2_{1/2}]$ as well); the pairs of layers obtained in both ways are geometrically equivalent. Among the infinite possible ordered or disordered sequences, there are two in which not only couples, but also triples (quadruples, ..., n–ples) of adjacent layers are geometrically equivalent. These are the so-called MDO (maximum degree of order) structures. In this case, we have two MDO polytypes (Fig. 2a). Polytype MDO1 results from a regular sequence of $n_{1/2,2}/n_{1/2,2}/n_{1/2,2}/....$operations (or $2_{-1/2}/2_{-1/2}/2_{-1/2}/.....$). In this case, the $n_{1/2,2}$ operation becomes a true n glide valid for the whole structure, with a translation $\mathbf{a} = 2\mathbf{a_0} + \mathbf{c}/2$. Moreover, the λ operation 2_1 and the σ operation $\bar{1}$ become total operations, valid for the whole structure. The resulting structure is monoclinic, space group $P12_1/a1$, with cell parameters $a_1 \approx 21.61$, $b_1 \approx 23.54$, $c_1 \approx 8.05$ Å and $\beta_1 \approx 100.7°$, and corresponds to the structure described by Mumme (1989). The twinned (100) counterpart can be derived in an analogous way, applying the sequence $n_{-1/2,2}/ n_{-1/2,2}/ n_{-1/2,2}/....$(or $2_{1/2}/2_{1/2}/2_{1/2}/.....$). The regular alternation of random blocks of the MDO1 and MDO1' polytypes gives rise to a polysynthetically twinned structure with a B-centered cell ($Bb2_1m$), which corresponds to the structure proposed by Born & Hellner (1960). The MDO2 results from the regular alternation of $n_{-1/2,2}/ n_{1/2,2}/n_{-1/2,2}/n_{1/2,2}/....$operations (or $2_{1/2}/2_{-1/2}/2_{1/2}/2_{-1/2}/.....$). In this case, the first and third layer are at the same level, and the λ operation n normal to $\mathbf{a_0}$ is continued through the whole structure, whereas the 2_2 σ operation becomes a 2_1 total operation, giving rise to a MDO polytype with space-group symmetry $P2_1/n11$ and cell parameters $a_2 \approx 21.24$, $b_2 \approx 23.54$, $c_2 \approx 8.05$ Å and $\alpha_2 \approx 90°$. Atomic coordinates for the MDO2 polytype can be derived from the positions of the family structure through the application of the matrix transformation [1 0 0/ 0 1 0/ 0 0 ½].

According to the nomenclature of polytypes recommended by the International Union of Crystallography (Guinier *et al*. 1984), the MDO1 and MDO2 polytypes should be denoted as boulangerite-2M_1 and boulangerite-2M_2, respectively, both presenting two layers within the unit translation $\mathbf{a}$.

The family structure is obtained by superposing Z copies of a general polytype of the family translated by the vector corresponding to the two possible positions of each OD layer (Fig. 2b). Assuming two basis vectors of the family structure collinear with the translation vectors $\mathbf{b}$ and $\mathbf{c}$ of the single layer, the vectors $\mathbf{A}$ $\mathbf{B}$ $\mathbf{C}$ of the family structure are such that: $\mathbf{A} = p\mathbf{a_0}$, $\mathbf{B} = \mathbf{b}/q$, and $\mathbf{C} = \mathbf{c}/t$, where q, t, and p are integers. In our case $q = 1$ and $t = 2$, whereas the number of layers, p, for the translation in the direction of the layer stacking can be obtained as the product of three factors $p =$

$p1\bullet p2\bullet p3$ (Dornberger-Schiff & Fichtner 1972), where $p1$ depends on the category of the OD structure, $p2$ depends on the isogonality relationships of operations in the OD-groupoid family symbol, and $p3$ depends on the Bravais lattice of the family structure (Ďurovič 1997, Ferraris *et al*. 2008). In the case under study, we have category Ia ($p1 = 1$), λ and σ operations, which are not isogonal ($p2 = 2$), and a P lattice ($p3 = 2$). As a consequence, in this family, p is equal to 2.

The space-group symmetry of the family structure can be derived by the λ and σ operations of the OD groupoid family symbol. In fact, the λ and σ operations are reflected in the symmetry operations of the family structure, once the translational components of any glide and screw are modified to take into account the different periodicities in passing from the single layer to the subcell. Therefore, we have to double the translational components that refer to the $\mathbf{c}$ axis and to divide by two the translational components that refer to the $\mathbf{a}$ axis in the OD groupoid family in order to obtain the operators:

$$
\begin{array}{ccc}
b & 2_1 & m \\
2_1 & n & 2_1
\end{array}
$$

which are the operators characterizing the space group $Pbnm$.

Therefore, the family structure has space group $Pbnm$ and translational vectors $\mathbf{A} = 2\mathbf{a_0}$, $\mathbf{B} = \mathbf{b}$, $\mathbf{C} = \mathbf{c}/2$, and corresponds to the structure obtained by Petrova *et al*. (1978a) and Skowron & Brown (1990a), as well as to the subcell structure derived by Born & Hellner (1960).

CHEMICAL COMPOSITION

The chemical composition of the boulangerite sample from Bottino investigated in this study was reported by Stasi *et al*. (1998). Electron-microprobe data were obtained with an ARL SEMQ–95 apparatus installed at the Centro Studi Geominerari e Mineralurgici, CNR, Cagliari. Operating conditions were: 20 kV and 20 nA. Standards and X-ray lines were: PbS (Pb $M\alpha$, S $K\alpha$), Sb_2S_3 (Sb $L\alpha$), Bi_2S_3 (Bi $M\alpha$), $FeAsS_2$ (As $L\alpha$), ZnS (Zn $K\alpha$), CuS (Cu $K\alpha$) and selenium (Se $L\alpha$). Detection limits (in wt.%) were: Pb 0.10, S 0.02, Sb 0.08, Bi 0.10, As 0.08, Zn 0.05, Cu 0.04, Se 0.04. The raw data were corrected with an on-line ZAF computer program. The results, obtained from eight-point analyses, show only minor variation from the ideal chemical composition of boulangerite. The sample analyzed is found to contain small amounts of Se (0.04–0.14 wt%), As (0.12–0.24 wt%) and Bi (0.10–0.24 wt%). The electron-microprobe results are reported in Table 1, together with chemical formulae calculated on the basis of 11(S, Se) atoms per formula unit. The chemical composition of another sample of boulangerite from Bottino described by Orlandi *et al*. (2008) also is reported for comparison.
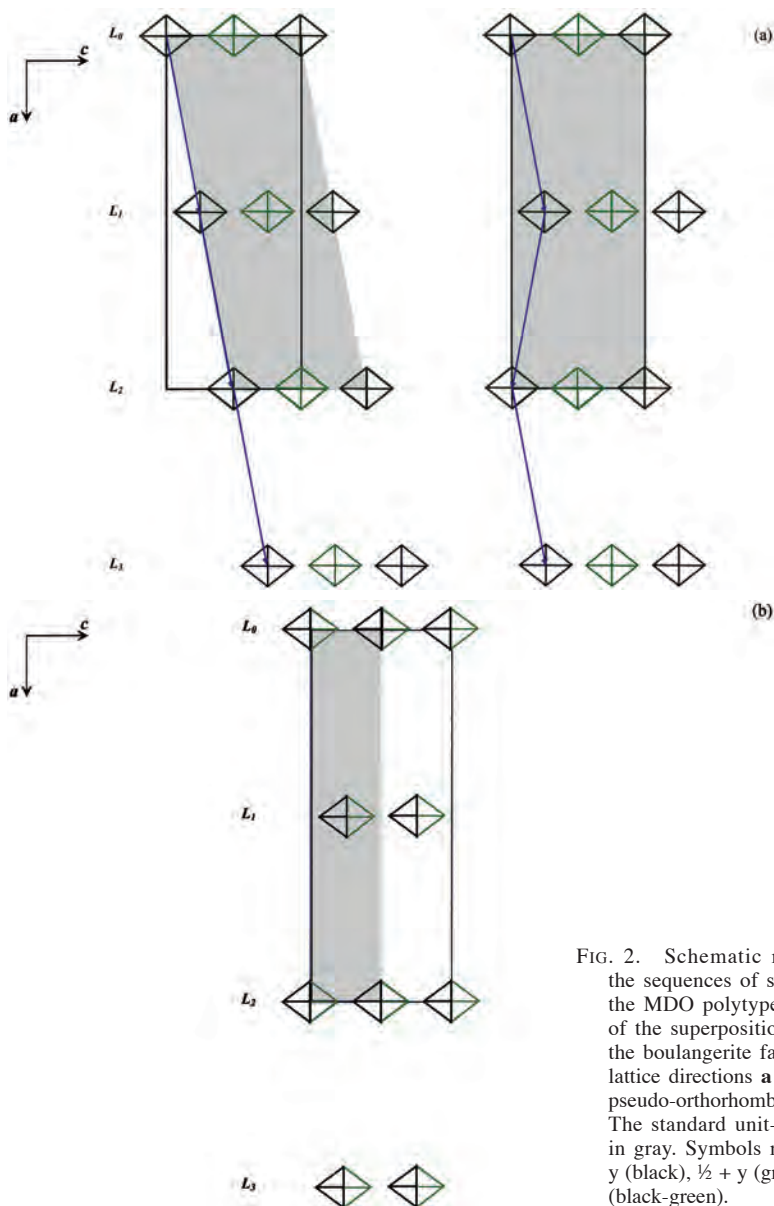
Fig. 2. Schematic representation of the sequences of structural layers in the MDO polytypes (a) and scheme of the superposition structure (b) of the boulangerite family. The crystal-lattice directions **a** and **c** refer to the pseudo-orthorhombic B-centered cell. The standard unit-cells are outlined in gray. Symbols represent atoms at y (black), ½ + y (green), and y, ½ + y (black-green).

X-RAY CRYSTALLOGRAPHY
AND CRYSTAL-STRUCTURE REFINEMENTS

Several crystals were mounted on a Bruker AXS X8 APEX II automated diffractometer, equipped with a CCD detector, with [001] direction parallel to the φ axis of the four-circle Kappa goniometer, and examined with graphite-monochromatized Mo $K\alpha$ radiation. After many trials, a single crystal suitable for the structural study was selected by examining a few sets of prelimi-nary frames. The collection strategy was optimized by the Apex suite of programs (Bruker 2003a); the intensities of reflections were recorded by a combina-tion of ω and φ rotation sets with a 0.5° scan width and a completeness of 99.8%, up to resolution 0.7 Å. The Miracol fiber optics capillary collimator (0.3 mm size) was used to enhance the intensity of the Mo$K\alpha$ radia-tion and to reduce the divergence of the X-ray beam. Data reduction, including intensity integration, correc-tion for Lorentz, polarization, background effects and

scale variation, was done using the package SAINT–IRIX (Bruker 2003b). A semi-empirical absorption correction (Blessing 1995) was performed using SADABS (Sheldrick 2008), and equivalent reflections were merged.

The X-ray-diffraction pattern displays strong sharp reflections for $l = 2n$, pointing to a primitive orthorhombic subcell with parameters a 21.170(4), b 23.470(4), c 4.0356(5) Å, plus a set of weak (sharp) reflections for $l = 2n + 1$. Including this second set of reflections, a new orthorhombic supercell with a 42.349(4), b 23.454(4), c 8.079 (2) Å could be indexed. Extinction conditions indicated a B-centered lattice, and $Bb2_1m$, $Bbm2$ and $Bbmm$ as possible space-groups. Taking into account the indications provided by the OD approach, the observed pattern was interpreted as a result of a polysynthetic (100) twin of alternating monoclinic individuals (MDO1 and MDO1') with space group $P2_1/a$ and cell parameters a 21.554(4), b 23.454(4), c 8.079(2) Å, β 100.76(1)°. The strong reflections (present only for $h = 2n$) were related to a periodic substructure, the 'family structure' (space group $Pbnm$). As a consequence, two refinement strategies were executed.

The first refinement was performed using the program CRYSTALS (Betteridge *et al.* 2003) starting from the atom coordinates of the orthorhombic subcell structure (Skowron & Brown 1990a). Refined parameters were: scale-factors, atom positions, site-occupancy factors, and anisotropic atomic-displacement factors. Only four sites showed mixed occupancy; they were allowed to vary their occupancies in the last cycles. A relatively anomalously large displacement-parameter was found for an Sb site. Accordingly, site splitting was introduced in the refinement, which lowered the R index from 6.80 to 4.77% (2701 reflections with $I > 3\sigma_I$).

The second refinement was carried out with the program SHELXL–97 (Sheldrick 1997) starting from the atom coordinates of the monoclinic structure studied by Mumme (1989) and assuming that (100) twinning is present. The introduction of this twin model through the matrix [101/010/00] improved the reliability R index from ~21 to ~8%, giving a ratio for the two twin components of 0.68:0.32. By analogy to Mumme's model, the cation sites A5 and A5' were first considered to be pure Pb and Sb sites, respectively. As the analysis of their coordination characteristics and bond-valence calculations suggested a mixed (Pb,Sb) occupancy for both of them, we attempted to refine A5 and A5' as mixed (Pb + Sb) sites. The two atomic species were refined with equal and isotropic displacement parameters, and the sum of occupancies was constrained to 1, but the coordinates were kept independent. The refined Pb:Sb ratio of scattering functions gave 0.69:0.31 and 0.46:0.54 for A5 and A5', respectively.

The final refinement with anisotropic displacement parameters for all cation and anion sites (except A5 and A5') converged to $R = 0.062$ [8495 reflections with $F_o > 4\sigma(F_o)$]. Scattering curves for neutrally charged atoms were used (Ibers & Hamilton 1974) in both refinements.

Although the absence of diffuse streaks parallel to **a*** for $l = 2n + 1$ suggests the lack of a significant proportion of fully disordered domains in our crystal, the possibility of stacking disorder was verified from the refinement. As family reflections are common to all ordered and disordered structures of the same OD structure, the occurrence in our crystal of completely disordered domains admixed with domains of the ordered MDO1 structure would be expected to lead to a systematic positive difference of hkl reflections having $l = 2n$ (family reflections) with respect to reflections having $l = 2n + 1$ (characteristic reflections of the MDO1 polytype). To eliminate the contribution of these potential disordered portions (the "Ďurovič" effect; Nespolo & Ferraris 2001), we attempted to refine the structure by using a separate scale-factor for the group of family reflections and the group of characteristic reflections. The relative scale-factors were varied in regular increments of 0.10, and the resulting R values from the structure refinements were compared. As the use of separate scale-factors for these two groups of reflections did not produce any improvement of the reliability index R, we concluded that the crystal examined is mostly characterized by ordered domains of the MDO1 polytype. Details about data collection and refinements are summarized in Table 2, together with crystal data. Fractional coordinates, site occupancies and displacement parameters

TABLE 1. CHEMICAL DATA OF BOULANGERITE FROM BOTTINO, APUANE ALPS, ITALY

No.	Pb	Sb	As	Bi	S	Se	Total	Ev[§]
1	53.95	26.29	0.15	0.10	18.64	0.04	99.17	1.1
2	54.62	26.26	0.13	0.14	18.80	0.06	100.01	0.6
3	54.27	26.43	0.22	0.24	18.82	-	99.98	1.1
4	53.92	26.35	0.13	0.17	18.70	0.06	99.33	0.8
5	54.28	27.08	0.17	-	19.01	0.09	100.63	0.8
6	53.95	26.89	0.12	0.11	18.87	0.14	100.08	0.8
7	54.73	26.88	0.24	0.10	18.96	0.08	100.99	1.4
8	53.97	26.70	-	-	18.90	0.13	99.70	-0.3
9*	55.60	24.02	1.74	-	19.16	-	100.52	
Mean	54.21	26.61	0.17	0.14	18.84	0.09	100.05	
St. dev.	0.32	0.32	0.05	0.05	0.12	0.04		0.61
Min.	53.92	26.26	0.12	0.10	18.64	0.04		
Max.	54.73	27.08	0.24	0.24	19.01	0.14		

Structural formulae based on S + Se = 11 *apfu*

1 $Pb_{4.92}(Sb_{4.08}As_{0.04}Bi_{0.01})_{\Sigma4.13}(S_{10.99}Se_{0.01})_{\Sigma11.00}$
2 $Pb_{4.94}(Sb_{4.04}As_{0.03}Bi_{0.01})_{\Sigma4.08}(S_{10.99}Se_{0.01})_{\Sigma11.00}$
3 $Pb_{4.91}(Sb_{4.07}As_{0.06}Bi_{0.02})_{\Sigma4.15}S_{11.00}$
4 $Pb_{4.90}(Sb_{4.08}As_{0.03}Bi_{0.02})_{\Sigma4.13}(S_{10.99}Se_{0.01})_{\Sigma11.00}$
5 $Pb_{4.85}(Sb_{4.12}As_{0.04})_{\Sigma4.16}(S_{10.98}Se_{0.02})_{\Sigma11.00}$
6 $Pb_{4.85}(Sb_{4.12}As_{0.03}Bi_{0.01})_{\Sigma4.16}(S_{10.97}Se_{0.03})_{\Sigma11.00}$
7 $Pb_{4.90}(Sb_{4.10}As_{0.06}Bi_{0.01})_{\Sigma4.17}(S_{10.98}Se_{0.02})_{\Sigma11.00}$
8 $Pb_{4.85}Sb_{4.08}(S_{10.97}Se_{0.03})_{\Sigma11.00}$
9* $Pb_{4.94}(Sb_{3.63}As_{0.43})_{\Sigma4.06}S_{11.00}$

Mean (anal. 1 – 8): $Pb_{4.89(3)}(Sb_{4.08(5)}As_{0.04(1)}Bi_{0.01})_{\Sigma4.13(6)}(S_{10.98(7)}Se_{0.02(1)})_{\Sigma11.00(8)}$.
Theoretical composition: $Pb_5Sb_4S_{11}$. [§] Equilibrium on the valence balance (Ev) calculated from the formula: [Σ(val⁺) – Σ(val⁻)] × 100 / Σ(val⁻).
* From Orlandi *et al.* (2008).

of the atoms in the structure of the MDO1 polytype are reported in Table 3, whereas selected bond-distances and bond-valence sums according to Brese & O'Keeffe (1991) are displayed in Table 4. The CIF file with structure data of the MDO1 polytype of boulangerite from Bottino can be downloaded from the *Inorganic Crystal Structure Database* at FIZ Karlsruhe, Germany (CSD number 423539). Tables containing fractional coordinates, occupancies and displacement parameters of atoms, and bond distances of the family structure, are available upon request from the authors and from the Depository of Unpublished Data on the Mineralogical Association of Canada website [document Boulangerite CM50_181].

DESCRIPTION OF THE CRYSTAL STRUCTURE

General features of the MDO1 polytype structure

The crystal structure of boulangerite from Bottino (Fig. 3) strongly resembles that of the monoclinic boulangerite with a close-to-ideal composition investigated by Mumme (1989). Geometrical features of these two structures are almost the same, but some differences were found in the values of atom coordinates, site populations and interatomic distances.

The main building-block of boulangerite involves lozenge-shaped rods of an SnS-like structure, infinite along [001] of the SnS archetype (Fig. 4). The arrangement of these rods results in rod-layers parallel to (100), characterized by a tightly bonded double-layer, crossing from one lozenge-shaped rod into another one *via* the constricted layer portion (Makovicky 1993). The latter represents a narrow part of the (100) rod-layers that connect adjacent lozenge-shaped rods and consists of the pair of square coordination-pyramids around the Pb sites A1 and A1'. Hence, boulangerite belongs to the family of rod-based layer sulfosalts composed of rods of SnS archetype (Makovicky 1993, Ferraris *et al.* 2008, Moëlo *et al.* 2008).

A rod-layer type geometrically similar to that of boulangerite (defined as Type 1 by Makovicky 1993)

TABLE 2. CRYSTAL, EXPERIMENTAL AND REFINEMENT DATA
FOR BOULANGERITE FROM BOTTINO

	Family structure	MDO1 polytype
Crystal data		
Structural formula	$Pb_{5.02}Sb_{3.98}S_{11}$	$Pb_{5.08}Sb_{3.93}S_{11}$
Cell setting, space group	Orthorhombic, *Pbnm*	Monoclinic, *P2₁/a*
a (Å)	21.170(4)	21.554(4)
b (Å)	23.470(4)	23.454(4)
c (Å)	4.0356(5)	8.079(2)
β (°)	---	100.76(1)
V (Å³)	2005.2(5)	4012(1)
Z	4	8
D (g cm⁻³)	6.22	6.21
Crystal habit	needle	
Crystal size (mm)	1.20 × 0.10 × 0.03	
Data collection		
Crystal–detector distance (mm)	60	
Rotation axes, width (°)	φ, ω, 0.5	
Exposure time (s/degree)	10	
No. of frames	3644	
Maximum covered 2θ (°)	61.16	
T_{min}, T_{max}	0.2986, 0.7461	
Reflections measured	57402	118995
Reflections unique	3940	12443
R_{nt}	0.086	0.156
Refinement		
R_1[a] (on F_o)	0.048	0.062
	(2701 with $I > 3\sigma_I$)	(8495 with $F_o > 4\sigma F_o$)
wR_2[b] (on F_o^2)	0.048	0.135
	(2701 with $I > 3\sigma_I$)	(8495 with $F_o > 4\sigma F_o$)
No. of refined parameters	131	360
Goof[c]	0.73	1.07
$\Delta\rho_{min}, \Delta\rho_{max}$ (e/Å³)	-6.42, 4.42	-6.04, 5.10

[a] $R_1 = \sum[||F_o| - |F_c||] / \sum|F_o|$. [b] $wR_2 = \{\sum[w(F_o^2 - F_c^2)^2] / \sum[w(F_o^2)^2]\}^{1/2}$, where $w = 1/[\sigma^2(F_o^2) + (0.0537\ P)^2 + 334.9155P]$. [c] Goodness-of-fit $= [\sum[w(F_o^2 - F_c^2)^2] / (N - P)]^{1/2}$, where N and P are the number of reflections and parameters, respectively.

TABLE 3. COORDINATES, DISPLACEMENT PARAMETERS (Å^2), AND OCCUPANCIES OF ATOMS IN MDO1 BOULANGERITE

Site	Atom	x/a	y/b	z/c	U_{eq}	U_{11}	U_{22}	U_{33}	U_{23}	U_{13}	U_{12}
A1	Pb	0.12228(5)	0.49872(4)	0.94540(18)	0.0228(2)	0.0302(5)	0.0160(4)	0.0233(6)	-0.0030(5)	0.0081(5)	-0.0029(3)
A2	Pb	0.30804(4)	0.15950(4)	0.02589(18)	0.01893(2)	0.0192(4)	0.0181(3)	0.0202(5)	0.0011(5)	0.0057(5)	-0.0013(3)
A3	Pb	0.20558(4)	0.32436(3)	0.97843(18)	0.0205(2)	0.0206(4)	0.0185(4)	0.0231(6)	0.0006(5)	0.0062(5)	0.0018(3)
A4	Sb	0.46610(8)	0.43755(7)	0.3338(3)	0.0215(4)	0.0200(8)	0.0153(6)	0.0291(12)	-0.0018(7)	0.0042(8)	-0.0024(5)
A5a	Pb 0.69(1)	0.13286(13)	0.09657(11)	0.2035(5)	0.0225(5)						
A5b	Sb 0.31(1)	0.1285(5)	0.1030(5)	0.200(2)	0.0225(5)						
A6	Sb	0.37145(7)	0.30864(6)	0.3090(3)	0.0164(3)	0.0172(6)	0.0124(6)	0.0195(9)	0.0016(7)	0.0032(8)	0.0001(5)
A7	Sb	0.05948(8)	0.23021(7)	0.8996(4)	0.0263(4)	0.0187(7)	0.0188(7)	0.0435(12)	0.0135(9)	0.0110(10)	0.0025(6)
A8	Sb	0.48592(7)	0.12122(6)	0.3615(3)	0.0148(3)	0.0200(7)	0.0084(5)	0.0173(9)	-0.0009(7)	0.0071(8)	-0.0010(5)
A9	Sb	0.29219(7)	0.45695(6)	0.2789(3)	0.0220(4)	0.0155(7)	0.0181(7)	0.0320(11)	-0.0006(9)	0.0033(9)	0.0001(5)
A1'	Pb	0.11178(5)	0.49911(4)	0.42704(19)	0.0245(2)	0.0372(5)	0.0151(3)	0.0228(6)	0.0000(5)	0.0092(6)	-0.0020(3)
A2'	Pb	0.30543(4)	0.15990(4)	0.52952(18)	0.01987(2)	0.0218(4)	0.0176(3)	0.0211(5)	-0.0001(5)	0.0062(5)	-0.0015(3)
A3'	Pb	0.20703(4)	0.32108(4)	0.4782(2)	0.0239(2)	0.0212(4)	0.0260(4)	0.0256(6)	0.0001(5)	0.0077(6)	0.0018(3)
A4'	Pb	0.45191(5)	0.42983(4)	0.84862(2)	0.0248(2)	0.0267(5)	0.0183(4)	0.0295(6)	0.0020(5)	0.0053(5)	0.0018(3)
A5a'	Pb 0.46(1)	0.13455(5)	0.09449(16)	0.6919(6)	0.0239(13)						
A5b'	Sb 0.54(1)	0.1262(16)	0.1049(3)	0.6779(9)	0.0239(13)						
A6'	Sb	0.38703(3)	0.28390(6)	0.8181(3)	0.0158(3)	0.0194(7)	0.0102(5)	0.0184(8)	0.0004(7)	0.0049(8)	-0.0026(5)
A7'	Sb	0.03872(5)	0.23296(4)	0.3978(2)	0.0268(2)	0.0276(5)	0.0159(4)	0.0359(6)	-0.0011(5)	0.0032(6)	-0.0023(3)
A8'	Pb	0.48697(4)	0.13465(4)	0.86647(18)	0.01921(2)	0.0231(4)	0.0122(3)	0.0231(5)	-0.0004(4)	0.0061(5)	0.0007(3)
A9'	Sb	0.28390(7)	0.46674(6)	0.7692(3)	0.0174(3)	0.0155(7)	0.0171(6)	0.0206(9)	-0.0002(8)	0.0061(8)	0.0012(5)
S1	S	0.0656(3)	0.0142(2)	0.8986(12)	0.0189(12)	0.014(3)	0.020(2)	0.024(4)	0.001(3)	0.005(3)	0.0007(18)
S2	S	0.1866(3)	0.4165(2)	0.2198(12)	0.0159(11)	0.015(2)	0.013(2)	0.020(3)	-0.002(3)	0.005(3)	-0.0022(17)
S3	S	0.2481(3)	0.0287(2)	0.0143(12)	0.0193(13)	0.022(3)	0.013(2)	0.025(4)	0.005(3)	0.008(3)	-0.001(2)
S4	S	0.0968(3)	0.2940(3)	0.1548(13)	0.0241(15)	0.017(3)	0.024(3)	0.033(5)	-0.003(3)	0.007(3)	-0.009(2)
S5	S	0.1569(3)	0.1729(2)	0.9512(14)	0.0253(14)	0.022(3)	0.010(2)	0.045(5)	-0.001(3)	0.010(4)	0.0034(19)
S6	S	0.3338(3)	0.3747(2)	0.0649(10)	0.0195(14)	0.022(3)	0.015(2)	0.022(4)	0.005(3)	0.006(3)	0.000(2)
S7	S	0.4180(3)	0.2218(2)	0.0690(10)	0.0155(12)	0.018(3)	0.013(2)	0.016(3)	0.003(3)	0.004(3)	-0.0028(18)
S8	S	0.0149(3)	0.4450(3)	0.1533(11)	0.0192(14)	0.018(3)	0.013(2)	0.029(4)	-0.001(3)	0.010(3)	-0.0044(19)
S9	S	0.3744(2)	0.0923(2)	0.3099(11)	0.0153(10)	0.012(2)	0.018(2)	0.015(3)	0.000(3)	0.002(3)	0.0025(18)
S10	S	0.2766(3)	0.2494(2)	0.2666(11)	0.0144(11)	0.019(3)	0.011(2)	0.016(3)	-0.002(3)	0.009(3)	-0.0012(17)
S11	S	0.0188(3)	0.1348(2)	0.1411(11)	0.0166(11)	0.021(3)	0.0107(19)	0.021(4)	0.003(3)	0.011(3)	0.0036(19)
S1'	S	0.0712(3)	0.0182(2)	0.4172(11)	0.0163(11)	0.017(2)	0.016(2)	0.016(3)	0.005(3)	0.003(3)	0.0042(18)
S2'	S	0.1866(3)	0.4120(2)	0.7164(11)	0.0166(11)	0.020(3)	0.015(2)	0.017(3)	0.001(3)	0.007(3)	0.0002(18)
S3'	S	0.2448(3)	0.0285(2)	0.4793(11)	0.0184(13)	0.016(3)	0.018(2)	0.021(4)	-0.004(3)	0.003(3)	0.000(2)
S4'	S	0.0951(3)	0.2938(2)	0.6960(11)	0.0215(15)	0.026(3)	0.015(3)	0.024(5)	0.006(3)	0.006(3)	-0.009(2)
S5'	S	0.1549(3)	0.1759(2)	0.4548(14)	0.0235(14)	0.012(2)	0.019(2)	0.041(4)	-0.008(4)	0.009(4)	0.0046(19)
S6'	S	0.3287(3)	0.3740(2)	0.5159(9)	0.0153(13)	0.020(3)	0.013(2)	0.015(4)	-0.003(2)	0.008(3)	0.0009(18)
S7'	S	0.4198(3)	0.2192(3)	0.6047(10)	0.0172(13)	0.017(3)	0.020(2)	0.017(4)	-0.002(3)	0.007(3)	-0.001(2)
S8'	S	0.0125(3)	0.4385(2)	0.6096(9)	0.0146(12)	0.019(3)	0.015(2)	0.011(3)	0.000(2)	0.004(3)	-0.0018(19)
S9'	S	0.3676(3)	0.0847(2)	0.8122(11)	0.0161(11)	0.020(3)	0.009(2)	0.020(3)	0.001(3)	0.008(3)	0.0045(17)
S10'	S	0.2769(3)	0.2510(2)	0.7614(11)	0.0155(11)	0.020(3)	0.014(2)	0.015(3)	0.001(3)	0.008(3)	0.0017(18)
S11'	S	0.0172(3)	0.1389(2)	0.6306(12)	0.0197(12)	0.018(3)	0.018(2)	0.025(4)	0.004(3)	0.008(3)	0.004(2)

is also present in the structures of robinsonite (Petrova *et al.* 1978b, Skowron & Brown 1990b, Makovicky *et al.* 2004) and of the synthetic compound $Pb_4Sb_6S_{13}$ (Jumas *et al.* 1980). However, the SnS-like rods of the boulangerite structure are actually "double rods", six atomic layers thick and three pyramids wide, in contrast to the thinner rods occurring in the latter two structures (Mumme 1989). The central portion of thick SnS-like rods of boulangerite is represented by ribbons of coordination pyramids of Pb and Sb atoms alternating along [001]. They will be defined as *ribbon C* in the following. The marginal portions are characterized by ribbons of coordination pyramids primarily occupied by Sb (hereafter defined as *ribbon M*). Considering the two additional weakly bonded S atoms under the base of the pyramids, the coordination environment of Pb and Sb sites in the rod interior has the form of a monocapped trigonal prism. The two largest Pb–S and Sb–S distances in these coordination polyhedra are influenced by the lone pairs of electrons of Sb atoms, that are accommodated in the interspaces between each couple of triple *ribbons C* and *M*, in the so-called lone-electron-pair micelles (Fig. 4).

The triple ribbon [100] of square coordination pyramids in the central portion of SnS-like rods (*ribbon C*) consists of (a) the marginal site A(Sb)7, which alternates with A(Pb)7' along [001], (b) a similar pair of alternating mixed sites A(Pb,Sb)5 and A(Sb,Pb)5' at the opposing margin of the ribbon, and (c) the central pair A(Sb)4 and A(Pb)4' (Fig. 5a). In the marginal

TABLE 4. SELECTED BOND-DISTANCES (Å) FOR MDO1 BOULANGERITE
WITH CORRESPONDING BOND-VALENCES (B.V.)*

	d (Å)	B.V.		d (Å)	B.V.		d (Å)	B.V.
A(Pb)1– S9'	2.791(7)	0.52	A(Pb)2– S7	2.750(6)	0.58	A(Pb)3– S6	2.966(6)	0.33
S3	2.840(6)	0.46	S9	2.927(7)	0.36	S2'	2.924(7)	0.36
S9	3.022(7)	0.28	S9'	2.921(8)	0.37	S4	3.047(9)	0.26
S2	3.067(7)	0.25	S10	3.030(7)	0.27	S2	2.990(7)	0.30
S8	3.200(6)	0.17	S10'	3.014(7)	0.29	S10	3.086(7)	0.24
S2'	3.231(7)	0.16	S5	3.216(6)	0.17	S10'	3.067(8)	0.25
S8'	3.544(6)	0.07	S3	3.323(5)	0.12	S4'	3.060(7)	0.25
S8	3.349(8)	0.12	Sum		2.16	S5	3.699(5)	0.05
Sum		2.03				Sum		2.03

	d (Å)	B.V.		d (Å)	B.V.		d (Å)	B.V.
A(Sb)4– S11	2.617(8)	0.64	A(Pb)5a– S5	2.833(10)	0.47	A(Sb)5b– S5	2.750(18)	0.44
S1'	2.468(6)	0.95	S5'	2.729(9)	0.62	S5'	2.655(17)	0.58
S1	2.597(8)	0.67	S11	2.716(7)	0.64	S11	2.581(12)	0.70
S11'	3.032(8)	0.21	S1	3.251(8)	0.15	S1	3.2971(15)	0.10
S1'	2.979(8)	0.24	S1'	2.997(8)	0.30	S1'	3.061(16)	0.19
S6	3.565(6)	0.05	S3	3.530(8)	0.07	S3	3.658(15)	0.04
S6'	3.845(7)	0.02	S3'	3.366(7)	0.11	S3'	3.509(14)	0.06
Sum		2.78	Sum		2.36	Sum		2.11

A(Pb)5a and A(Sb)5b: BVS site§ = 2.28; theoretical BVS: 2.31

	d (Å)	B.V.		d (Å)	B.V.		d (Å)	B.V.
A(Sb)6– S10	2.442(6)	1.02	A(Sb)7– S5	2.462(6)	0.97	A(Sb)8– S9	2.457(5)	0.98
S6'	2.563(7)	0.74	S4'	2.448(8)	1.01	S8	2.454(8)	0.99
S6	2.520(7)	0.83	S4	2.553(9)	0.76	S8'	2.425(7)	1.07
S7	3.105(7)	0.17	S11	3.259(8)	0.11	S7	3.464(6)	0.07
S7'	3.204(8)	0.13	S11'	3.066(8)	0.19	S7'	3.495(6)	0.06
S11	3.779(8)	0.03	S7'	3.670(7)	0.04	S4'	3.800(7)	0.03
S11'	3.884(7)	0.02	S7	3.741(8)	0.03	S4	3.734(9)	0.03
Sum		2.94	Sum		3.11	Sum		3.23

	d (Å)	B.V.		d (Å)	B.V.		d (Å)	B.V.
A(Sb)9– S2	2.429(6)	1.06	A(Pb)1'– S9'	2.878(7)	0.41	A(Pb)2'– S7'	2.797(7)	0.51
S3	2.903(8)	0.29	S3'	3.119(6)	0.22	S9	2.976(7)	0.32
S3'	2.802(8)	0.39	S9	3.024(7)	0.28	S9'	2.997(7)	0.30
S6	2.845(7)	0.34	S2	3.291(7)	0.14	S10	2.968(7)	0.32
S6'	2.740(6)	0.46	S8'	3.155(7)	0.20	S10'	2.981(7)	0.31
S1	3.860(8)	0.02	S2	3.189(7)	0.18	S5'	3.209(6)	0.17
S1'	3.750(7)	0.03	S8'	3.018(6)	0.28	S3'	3.342(5)	0.12
Sum		2.59	S8	3.023(7)	0.28	Sum		2.05
			Sum		1.99			

	d (Å)	B.V.		d (Å)	B.V.		d (Å)	B.V.
A(Pb)3'– S6'	2.866(6)	0.43	A(Pb)4'– S11	2.900(7)	0.39	A(Pb)5a'– S5	2.762(10)	0.56
S2'	2.960(7)	0.33	S1	2.918(8)	0.37	S5'	2.797(10)	0.51
S4	3.249(8)	0.15	S1	2.743(6)	0.59	S11'	2.694(7)	0.68
S5'	3.580(5)	0.06	S11'	2.934(8)	0.35	S1	3.077(9)	0.24
S10	2.992(8)	0.30	S1'	2.959(7)	0.33	S1'	2.977(8)	0.32
S10'	2.986(7)	0.31	S6	3.587(8)	0.06	S3	3.574(8)	0.06
S4'	3.303(8)	0.13	S6'	3.651(6)	0.05	S3'	3.538(9)	0.07
S2	3.036(7)	0.27	Sum		2.14	Sum		2.44
Sum		1.98						

	d (Å)	B.V.		d (Å)	B.V.		d (Å)	B.V.
A(Sb)5b'– S5	2.704(12)	0.50	A(Sb)6'– S10'	2.456(6)	0.98	A(Pb)7'– S5'	2.801(6)	0.51
S5'	2.612(12)	0.65	S6'	3.296(6)	0.10	S4'	2.868(7)	0.42
S11'	2.443(9)	1.02	S6	3.268(7)	0.11	S4	2.896(10)	0.39
S1	3.206(11)	0.13	S7	2.484(7)	0.91	S11	3.080(7)	0.24
S1'	3.007(10)	0.22	S7'	2.496(8)	0.88	S11'	2.991(8)	0.30
S3'	3.722(10)	0.03	S11	3.880(7)	0.02	S7'	3.496(8)	0.08
S3	3.849(9)	0.02	S11'	3.877(8)	0.02	S7	3.517(7)	0.07
Sum		2.57	Sum		3.02	Sum		2.01

A(Pb)5a' and A(Sb)5b': BVS site§ = 2.51; theoretical BVS = 2.54

	d (Å)	B.V.		d (Å)	B.V.
A(Pb)8'– S9'	2.786(6)	0.53	A(Sb)9'– S2'	2.428(6)	1.06
S8	2.950(7)	0.34	S3	2.469(9)	0.95
S8'	2.825(7)	0.48	S3'	2.459(8)	0.98
S7	3.158(7)	0.19	S6	3.250(7)	0.12
S7'	3.059(7)	0.25	S6'	3.254(7)	0.11
S4'	3.368(7)	0.11	S1	3.964(7)	0.02
S4	3.431(8)	0.09	S1'	3.903(8)	0.02
Sum		1.99	Sum		3.26

* Calculated according to Brese & O'Keeffe (1991). § Mean of BVS (bond-valence sum, expressed in valence units) according to the fractional occupancies reported in Table 3.
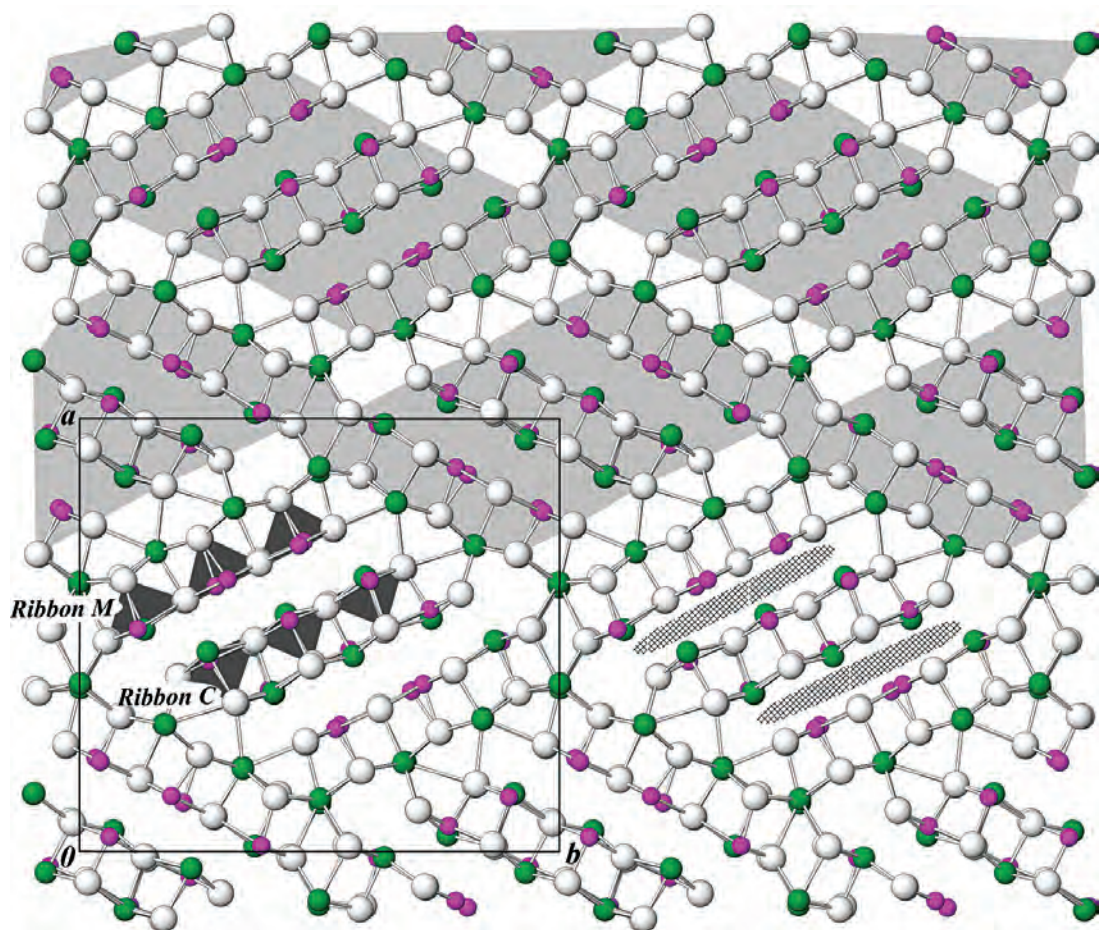
coordination pyramids, the two basal Sb–S and Pb–S distances pointing toward the center of the ribbons are longer, and those pointing outward, toward the edge of the ribbons, are shorter. A similar characteristic was also observed in the Sb ribbons of the jamesonite structure (Makovicky 1993, Ferraris *et al.* 2008). In the central [001] row with alternating A(Sb)4 and A(Pb)4' atoms, the shorter pair of Sb–S bonds in the bases of the Sb coordination pyramids are oriented upward along the infinite [001] rod axis, whereas the longer pairs are oriented downward; an opposite scheme is observed for pairs of short and long bonds in the bases of Pb coordination pyramids (Fig. 5a).

The triple ribbon with marginal sites A(Sb)9 and A(Sb)9', central sites A(Sb)6 and A(Sb)6', and again marginal sites A(Sb)8 and A(Pb)8' (*ribbon M*) consists

of trapezoidally distorted "square" coordination pyramids (Fig. 5b). The shorter and longer pair of Sb–S bonds in the trapezoidal bases of the coordination pyramids are alternatively directed toward the right and left in each [001] central row A(Sb)6 – A(Sb)6' – A(Sb)6. According to Mumme (1989), this behavior is similar to that observed in the pure Sb rows comprising the octahedra of the "galena-like" slabs that surround a central micelle, in the structure of ramdohrite (Makovicky & Mumme 1983). Atom A(Sb)6', with its two short A(Sb)6'–S7 and A(Sb)6'–S7' bonds, forces the adjacent site A(Pb)8' into a trapezoidal and eccentric coordination, with the central cation displaced toward the longer base of the trapezoid (Fig. 5b). In the marginal pure Sb row with alternating A(Sb)9 and A(Sb)9' atoms, the distribution of short Sb–S bonds in

FIG. 3.   The crystal structure of the polytype MDO1 of the boulangerite family projected on (001). In order of decreasing size, spheres represent S atoms (white), Pb atoms (green) and Sb atoms (pink).

Fig. 4.   Projection of the crystal structure of boulangerite along [001]. Upper side: lozenge-shaped rod-layers (100) of the SnS-
like archetype (shaded gray) and non-commensurate interspaces between them (unshaded). Lower side: lone electron-pair
micelles (cross-hatched) and ribbons of coordination pyramids of Sb and Pb (shaded dark gray).

the trapezoidal array forms fragments of the so-called
Sb–S crankshaft chains described for members of the
sartorite homologous series (Berlepsch *et al*. 2001a).

Lozenge-shaped rods of the structure are limited by
two opposing surfaces that display a pseudohexagonal
motif of S atoms on one side (H surfaces in Makovicky
1981) and by surfaces displaying a pseudotetragonal
motif of S atoms on the other two opposing sides (Q
surfaces in Makovicky 1981). Consequently, a non-
commensurate fit occurs between pseudotetragonal,
Pb-rich surface (Q) of one rod and the pure-anion pseu-
dohexagonal surface (H) of the opposing rod.

Square coordination-pyramids of Pb occurring on
the Q surfaces form part of variously capped trigonal
coordination-prisms of Pb, which span the non-
commensurate interspaces between adjacent rod-layers
(Fig. 4).

Coordination polyhedra in the MDO1
polytype structure

There are two types of lead sites in boulangerite.
The first consists of mono- and bicapped trigonal pris-
matic coordinated sites along the surface of structural
rods, *i.e*., A(Pb)1, A(Pb)1', A(Pb)2, A(Pb)2', A(Pb)3,
A(Pb)3', and the second consists of Pb sites alter-
nating with Sb in triple ribbons of Sb–Pb coordination
pyramids, *i.e*., A(Pb)4', A(Pb)7', A(Pb)8', mixed sites
A(Pb,Sb)5 and A(Sb,Pb)5'.

The coordination prisms around Pb sites A1, A3,
A1' and A3' are distorted "standing" bicapped trigonal
prisms with the (approximate) three-fold axis parallel
to [001], and those around Pb sites A2 and A2' are
"lying" monocapped trigonal prisms with the axis
perpendicular to [001]. The position of Pb atoms inside

lying monocapped trigonal coordination prisms is very eccentric, with the set of Pb–S distances across the rod interspace distinctly longer than the others. Moreover, in each coordination prism, the central cation-to-cap distance is shorter than the distances of the cation to the S atoms at the two opposing bases of the prism (Table 4). The above evidence suggests that these Pb atoms display an active pair of lone electrons. In bicapped trigonal coordination prisms of A(Pb)1' and A(Pb)3, the Pb–S distances at the bases of the prisms are of almost uniform length, whereas the corresponding sites at $z \approx 0$ and $z \approx 0.5$ Å, *i.e.*, A(Pb)1 and A(Pb)3', show a more asymmetric trigonal prismatic environment, with one set of Pb–S distances considerably longer than the other bonds of the coordination prisms (Table 4). These weak interactions correspond to the bonds formed by A(Pb)1 and A(Pb)3' to S atoms shared respectively with ribbon sites A(Pb)8' and A(Pb)7'. One should note that the distances of the same S atoms to the cation sites A(Pb)1' and A(Pb)3, alternating respectively with A(Pb)1 and A(Pb)3'along [001], are significantly

shorter, if Sb occurs in the closer ribbon sites [*i.e.*, A(Sb)8 and A(Sb)7] instead of Pb.

In the bicapped trigonal coordination prisms described above, the distances of each capping S atom from the central cation represent, respectively, one of the shortest and one of the longest Pb–S distances of the whole coordination polyhedra.

The Pb sites alternating with Sb in the Pb-rich *ribbons C* and the only Pb site in the *ribbon M*, richest in Sb, show a square pyramidal coordination, with Pb–S distances ranging from 2.743(6) to 3.158(7) Å; the bridging distances to the additional S atoms under the base of the coordination pyramids range from 3.368(7) to 3.651(6) Å.

In the coordination polyhedra around pure Sb sites A6, A7, A8, A6', A9', three short bonds [2.425(7) – 2.563(7) Å] are combined with four long distances, starting at 3.066(8) Å or, for A(Sb)8', even at 3.464 Å (Table 4). With the exception of A(Sb)7, all these Sb atoms belong to the *ribbon M* and form [SbS₅] coordination pyramids with trapezoidal bases (Fig. 5b). The
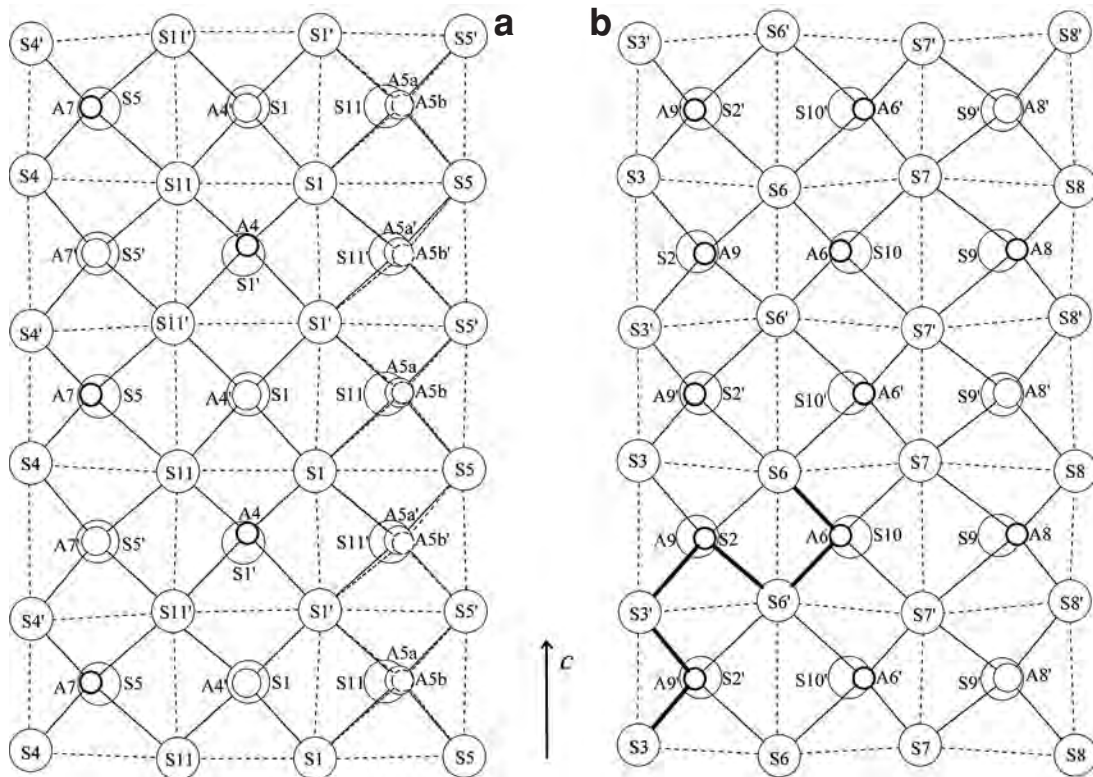

FIG. 5.   Ribbons of Sb and Pb atoms projected perpendicular to [001]; in order of decreasing size, the circles represent S, Pb and Sb atoms. (a) Plane of the *ribbon C* with square bases of the distorted coordination pyramids [SbS₅] and [PbS₅]. (b) Plane of the *ribbon M* with trapezoidal bases of the distorted "square" coordination pyramids [SbS₅] and [PbS₅]; a fragment of Sb–S-crankshaft chains (Berlepsch *et al.* 2001a) is outlined on the bottom-left side.

two longest Sb–S distances span the lone-electron-pair micelle that separates a triple *ribbon C* from *M*.

The pure Sb position A4 shows a square pyramidal coordination, with a short Sb–S distance to the apex of the pyramid equal to 2.468(6) Å, and minor differentiation between stronger and weaker pairs of opposing bonds in the base of the pyramid with respect to the Sb coordinations described above. Hence, its shorter basal bonds are slightly longer than those in the other Sb coordination pyramids, whereas its longer basal bonds are slightly shorter. This feature may be explained considering that the A(Sb)4 coordination polyhedron lies in the center of *ribbon C*, surrounded by edge-sharing coordination pyramids of Pb along the extension of the ribbon ([001]) and in the direction perpendicular to it.

An even more anomalous coordination can be observed for the Sb site A9. In this case, the two shorter bonds in the base of the coordination pyramid are too large for a pure Sb site, and their differentiation with respect to the opposing distances is still minor compared to that observed for the pair of short-to-opposing-long distances in the base of the coordination pyramid of A(Sb)4. The two almost equally large basal Sb–S distances, which resemble closely the opposing longer bonds [2.740(6) and 2.802(8) Å *versus* 2.903(8) and 2.845 Å, respectively], suggest a possible Pb-for-Sb replacement at A(Sb)9. Note that this hypothesis seems to be confirmed by the significant deficit of valences observed at this site (Table 4). However, the value of the short apical bond is consistent with a pure Sb site. As the refinement with mixed (Sb,Pb) occupancy at A9 suggests very minor percentage of Pb for Sb substitution, a full Sb occupancy was assumed in the final refinement.

In Figure 6, the element-specific bond-length hyperbolae taken from Berlepsch *et al.* (2001a) are reported, with pair of opposing *Me*–S distances from Sb and Pb coordination polyhedra of boulangerite added. Pairs of *Me*–S distances in the base of the pyramids are plotted in the space above the median line, whereas the pairs of opposing bonds perpendicular to the base of the pyramids are plotted in the space below this line. Owing to the occurrence in SnS-like rods of two additional S atoms under the base of the coordination pyramids in the rod interior, an ambiguity between two candidates is present in the choice of the long weak bond opposing the short bond to the apex of the pyramids. The criteria used here for selecting these bond-pairs are those illustrated in Berlepsch *et al.* (2001a, 2001b). The diagram shows that cation-to-ligand distances in coordination polyhedra of pure Sb sites A6, A7, A8, A6', A9' follow the hyperbolic trend established for Sb by Berlepsch *et al.* (2001a), and those of pure Pb sites A4', A7' and A8' plot almost perfectly on the Pb bond-length hyperbola. On the contrary, some deviations were observed for bond distances in coordination polyhedra of the pure Sb sites A4 and A9 and mixed sites A(Pb,Sb)5 and

A(Sb,Pb)5'. The deviation from the Sb hyperbola of pair of bonds in A(Sb)4 and A(Sb)9 coordination polyhedra follows a straight trend similar to that already observed by plotting bond lengths from the structures of dadsonite (Makovicky *et al.* 2006) and of some Pb–As sulfosalts (Berlepsch *et al.* 2001b). According to Makovicky *et al.* (2006) and Berlepsch *et al.* (2001b), this kind of trend is typical of split positions. A similar conclusion arises also from bond-valence calculations, which show anomalously low sums for sites A4 and A9 with respect to the other Sb sites (Table 4). However, no evidence of splitting for the two sites A4 and A9 resulted from U_{ii} values, as well as from the Fourier map, and consequently, both these two cation positions were left unsplit in the structure refinement.

Data points for the mixed sites A(Pb,Sb)5 and A(Sb,Pb)5' lie, instead, on hyperbolae intermediate between those of Sb and Pb, reflecting the fact that all the S positions involved are the average of S positions belonging to the Sb-occupied and Pb-occupied versions of the same mixed-cation polyhedron. Deviations from the hyperbolic relationship were also observed for pairs of opposing bond-lengths in bicapped trigonal coordination prisms of A(Pb)1 and A(Pb)1'. Note that hyperbolic relationships in the trigonal coordination prisms are never perfect as a consequence of approximations to the octahedral model (Berlepsch *et al.* 2001a, 2001b).

Comparison between family structure and MDO1 polytype structure

The structure refinements of the ordered MDO1 polytype and of the OD family structure of boulangerite performed in the current study using the same set of X-ray data allow a careful comparison between details of cation distribution and bonding scheme in these two structures. The family structure of boulangerite refined here shows the occurrence of several mixed (Pb,Sb) sites residing, with the exception of A(Pb,Sb)8, in the central, tightly bonded slab of the large SnS-like rods, six atom planes thick. These mixed sites do not indicate a true chemical disorder. In fact, as in OD structures, the family structure is formed by the superposition of individual layers from all possible ordered and disordered structures of the same OD family; these mixed sites arise from the overlapping of the regularly alternating Sb and Pb cation sites of the ordered structure into one 4 Å layer structure. The refined occupancies showing almost equal amounts of Pb and Sb in each mixed site attest to this. Note that for the site A(Pb,Sb)5 of the 4 Å structure, the refined Pb:Sb ratio is close to the mean value between Pb:Sb ratios from the corresponding pair of alternating sites A(Pb,Sb)5 and A(Sb,Pb)5' (Pb:Sb = 0.69:0.31 and 0.46:0.54, respectively) in the ordered MDO1 structure. Furthermore, it can be noted that cation-to-ligand distances in coordination polyhedra of mixed (Sb,Pb) sites of the family structure are close to
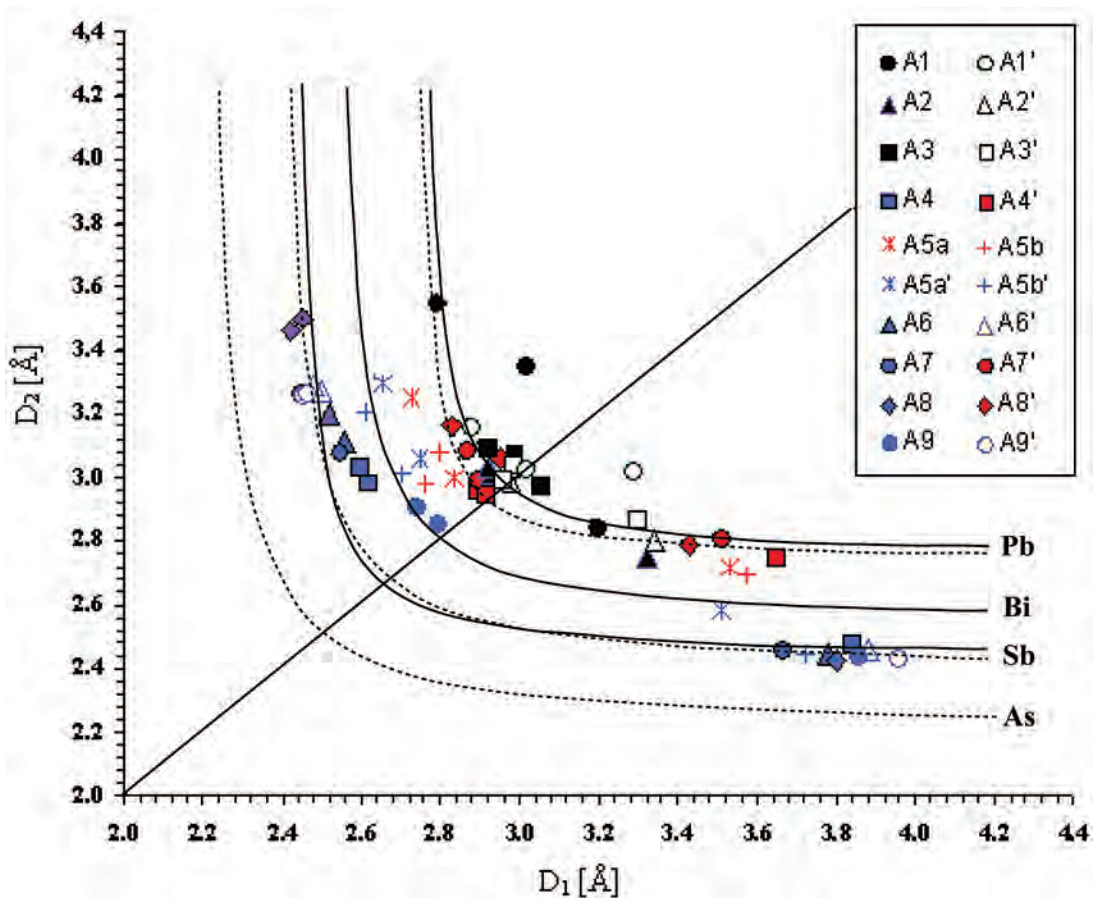
Fɪɢ. 6.　Element-specific bond-length hyperbolae for the pairs of opposing bonds (Berlepsch *et al.* 2001b), with individual Pb–S and Sb–S distances of coordination polyhedra of boulangerite added. The upper-left-hand part of the diagram contains pairs of bonds from the bases of trapezoidal and square distorted coordination pyramids; the lower-right-hand side comprises bonds to the vertex of the coordination pyramids, opposed by the shortest cation–anion distance below the base of the pyramid. The definition of pairs of bond lengths in coordination polyhedra of A1, A1', A3, A3' sites is only tentative, as they are bicapped trigonal prisms.

the mean values between analogous distances for pairs of alternating Sb and Pb coordination polyhedra in the corresponding columns of the ordered structure.

No partial Pb-for-Sb substitution resulted for the two sites A(Sb)6 and A(Sb)9 of the family structure, which are pure Sb sites in the ordered MDO1 structure as well. Nevertheless, the overlapping character of these sites is shown by their bonding scheme. As a matter of fact, the Sb–S distances in the base of the coordination pyramid around A(Sb)9 are an average of the corresponding pairs of basal distances from coordination polyhedra of alternating sites A(Sb)9 and A(Sb)9' in the MDO1 structure. Besides, the split of the site A(Sb)6 into two partly occupied Sb positions inside the same coordination polyhedron can be attributed to the overlapping in

this average structure of the two regularly alternating sites A(Sb)6 and A(Sb)6' of the ordered MDO1 structure, which are displaced respectively toward the left and right side of the *ribbon M* (Fig. 5b). Note also that *ribbon M* of the family structure shows a square array of S atoms resulting from the superposition of S atoms that belong to the trapezoidal bases of two oppositely oriented coordination pyramids in the MDO1 structure.

Neither statistical splitting nor partial Sb-for-Pb substitution is observed in the pure Pb sites of the family structure; each of them is an average of two very similar Pb coordination polyhedra from the ordered MDO1 structure.

Except for fine details, the family structure refined here shows general agreement with the subcell struc-

tures of boulangerite reported by Born & Hellner (1960) for a sample from Příbram, Bohemia, and by Petrova *et al.* (1978a) and Skowron & Brown (1990a) for synthetic crystals. The largest differences are observed in the split site A(Sb)6 and in the occupancy factors of mixed (Pb,Sb) sites (Table 5). Both Petrova *et al.* (1978a) and Skowron & Brown (1990a) did not take into account the splitting of A6, although this seems highly advisable according to the published structural data. As a matter of fact, in both refinements, such splitting seems indicated by the higher values of the displacement parameter for this site with respect to those of the other similar sites. Furthermore, splitting is confirmed by the bonding scheme of this cation site, which shows a short distance to the apex of the pyramid in good agreement with a pure Sb site, but two pairs of opposing Sb–S distances in the base of the pyramid, which are not consistent with Sb. It can be noted that the latter match very well the mean value between pairs of corresponding distances in coordination polyhedra of alternating A(Sb)6 and A(Sb)6' sites in the MDO1 structure. A similar coordination consisting of two split "half-atoms" biased asymmetrically each to its side of a pyramid is also present in the structures of dadsonite (Makovicky *et al.* 2006) and of the unnamed natural phase $Pb_{15-2x}Sb_{14+2x}S_{36}O_x$ (Makovicky & Topa 2009).

In our study, the occupancies were determined from the structure refinement, leading to the well-balanced formula $Pb_{5.02}Sb_{3.98}S_{11}$. The model proposed by Born & Hellner (1960) shows a statistical distribution of Pb and Sb over three sites, three pure Sb sites and three pure Pb sites (Table 5), pointing to a composition expressed by the unbalanced chemical formula $Pb_{4.5}Sb_{4.5}S_{11}$. The refined structure of Petrova *et al.* (1978a) displays four mixed sites with almost statistical distribution of Sb and Pb, which gives the ideal charge-balanced formula $Pb_5Sb_4S_{11}$. Finally, the model with four mixed sites proposed by Skowron & Brown (1990a) shows occu-

pancy numbers significantly different from ours and from those reported by Petrova *et al.* (1978a). However, the cation distribution reported by Skowron & Brown (1990a) was obtained from bond-valence calculations, as the site-occupancy factors obtained from least-squares refinement of X-ray data produced the formula $Pb_{4.65}Sb_{4.35}S_{11}$, significantly different from the expected electrostatically neutral formula $Pb_5Sb_4S_{11}$.

DISCUSSION AND CONCLUSIONS

Although boulangerite has been the object of several structural studies, several questions concerning its crystal structure had not been adequately addressed to date. In particular, a general confusion regarding the existence of monoclinic structures with an ordered distribution of Pb and Sb atoms and orthorhombic structures with mixed (Pb,Sb) sites into the SnS-like rods persisted in previous studies. The careful application of OD procedures performed in this work gives a comprehensive insight of all crystallographic features of boulangerite, allowing us to clarify relationships between monoclinic and orthorhombic structures reported in the literature on this mineral.

Taking into account the indication given by the OD theory, we carried out an accurate refinement of the ordered monoclinic polytype MDO1 of boulangerite (cell parameters *a* 21.554(4), *b* 23.454(4), *c* 8.079(2) Å, β 100.76(1)°, space group $P2_1/a$). Besides, it was possible for us to ascertain that the symmetry of the orthorhombic supercell displayed in our diffraction pattern and already observed in previous studies (Born & Hellner 1960), can be referred to (100) twinning, giving rise to a B-centered pseudorhombic cell with parameters *a* 42.349(4), *b* 23.454(4), *c* 8.079(2) Å. The structure refinement showed a ratio for the two twin components equal to 0.69:0.31, which suggests a crystal composed of a large number of twin domains.

TABLE 5. DISTRIBUTION OF Pb AND Sb IN CATION SITES OF THE FAMILY STRUCTURE
OF BOULANGERITE FROM BOTTINO AND COMPARISON WITH LITERATURE DATA

Sites	This study		Born & Hellner (1960)		Petrova *et al.* (1978a)		Skowron & Brown (1990a)	
	Pb	Sb	Pb	Sb	Pb	Sb	Pb	Sb
A1	100	0	100	0	100	0	100	0
A2	100	0	100	0	100	0	100	0
A3	100	0	100	0	100	0	100	0
A4	48.53(8)	51.47(8)	50	50	45	55	64	36
A5	53.53(8)	46.48(8)	50	50	60	40	62	38
A6a	0	50	0	50	0	100	0	100
A6b	0	50	0	50	-	-	-	-
A7	51.34(8)	48.66(8)	0	100	50	50	30	70
A8	48.21(8)	51.80(8)	50	50	45	55	44	56
A9	0	100	0	100	0	100	0	100
Structural formula	$Pb_{5.02}Sb_{3.98}S_{11}$		$Pb_{4.5}Sb_{4.5}S_{11}$		$Pb_{5.00}Sb_{4.00}S_{11}$		$Pb_{5.00}Sb_{4.00}S_{11}$	

This result is in agreement with findings of Dornberger-Schiff & Höhne (1962), who described a diffraction pattern characterized by some areas displaying monoclinic symmetry and some areas with orthorhombic symmetry for a seemingly monocrystalline specimen of boulangerite.

The structural model of the MDO1 polytype obtained in the present refinement is characterized by 18 independent cation sites, of which 10 are pure lead sites, six are pure antimony sites, whereas two cation sites are mixed positions split into two close sites occupied by Pb and Sb, respectively. Except for minor but significant differences concerning coordinates, bond distances and occupancy values of the atoms, the model obtained is similar to that described by Mumme (1989). The major difference between these two structures concerns the occurrence in our structure of the mixed (Pb,Sb) sites A5 and A5', with a Pb:Sb ratio of scattering functions of 0.69(1):0.31(1) and 0.46(1):0.54(1), respectively; in Mumme's model, they were assumed to be pure Pb and pure Sb sites, respectively.

The presence of mixed (Pb,Sb) sites in the monoclinic structure refined here attests to a limited Pb:Sb solid-solution behavior inside the ribbons of the MDO1-ordered domains of boulangerite, which, however, preserve the boulangerite stoichiometry. This result is in agreement with the findings of Mumme (1989), who stated that in Sb–Pb–Sb [001] columns of boulangerite, the incorporation of extra Pb in place of an equal amount of Sb cannot be possible owing to charge-balance requirements. It should be stressed that an analysis of coordination environments and valence sums calculated for cation sites in the structure reported by Mumme (1989) suggests the presence of several mixed (Pb,Sb) sites, which were not considered by him, but which, as in our case, do not cause a significant deviation from the ideal composition of boulangerite.

The orthorhombic subcell structure with lattice parameters a 21.170(4), b 23.470(4) and c 4.0356(5) Å, space group $Pbnm$ (or the so-called "family structure" in accordance with the OD nomenclature; Dornberger-Schiff 1964, 1966, Ďurovič 1997, Ferraris et al. 2008) refined in this study gives a disordered structural model, with several mixed-cation sites showing almost statistical distribution of Sb and Pb. Except for minor discrepancies, which were extensively discussed in the previous paragraphs (see *Comparison between family structure and monoclinic MDO1 structure*), the structure refinement of the *family structure* of boulangerite from Bottino reveals a model substantially similar to the subcell structure obtained by Born & Hellner (1960), Petrova et al. (1978a) and by Skowron & Brown (1990a).

In the last two works, which were based on the analysis of synthetic crystals, no mention of the occurrence of superstructure reflections was made. From the absence of diffuse lines, anomalies in the symmetry and extraneous spots in their X-ray data, Petrova et al. (1978a) concluded that superlattice ordered variants of boulangerite are present only in the natural specimens and that their synthetic crystals show a completely disordered structure with purely statistical solid solution involving Sb and Pb. However, electron-diffraction images obtained by Mozgova et al. (1983) from both natural and synthetic crystals of boulangerite (the same material used for the solution of the crystal structure by Petrova et al. 1978a), revealed the occurrence of very weak reflections with $l = 2n + 1$, corresponding to $c = 2 c' \approx 8$ Å, in addition to strong reflections with $l = 2n$, corresponding to $c' \approx 4$ Å. According to the above authors, odd reflections from the crystal lattice of the synthetic material were so weak that they were nearly unnoticeable in some electron-diffraction images, suggesting that they were probably undetectable in the X-ray diffraction data investigated by Petrova et al. (1978a).

In spite of these findings, a general diffuse confusion about the presence of ordered and disordered variants of boulangerite structure has remained in the literature. The possibility of extensive Pb–Sb exchanges at the sites of boulangerite was one of the bases for the proposal of the *boulangerite homologous series* (Mozgova et al. 1983). This concept, however, was definitively discredited by Mumme (1989). Furthermore, Bente & Anton (1995) inferred that ordered variants and OD phenomena occurring in natural samples of boulangerite are related to the Pb–Sb order, whereas a statistical distribution of metal cations can be observed in high-temperature synthetic boulangerite; on the basis of this assumption, they suggested to use the temperature dependency of metal-ordering schemes in this mineral as a potential geothermometer. However, their conclusion derives from a misinterpretation of the 4 Å substructure as a kind of statistical structure. As we have demonstrated in this work, the subcell structure refined by Petrova et al. (1978a) and Skowron & Brown (1990a) actually corresponds to the *family structure* of the boulangerite OD family, which is common to all possible ordered and disordered modifications that boulangerite may have in relation to the different conditions of crystallization. In agreement with the basic statement of the OD theory, it corresponds to a "fictitious structure" formed by the superposition of individual layers in all possible positions corresponding to all stacking vectors of this OD family; thus its chemical disorder also is fictitious. According to the OD theory, it is possible to expect the existence in nature of boulangerite crystals with completely disordered domains built up from a non-periodic stacking sequence of the OD boulangerite layer with symmetry $P(n)2_1m$. However, in that case, the X-ray-diffraction pattern should be characterized by more or less diffuse spots with $l = 2n +1$ in addition to sharp and strong maxima with $l = 2n$. As reported in the paragraph on experimental results, no evidence of disordered stacking sequences is present in the boulangerite crystal examined from Bottino, which is

characterized only by ordered domains of the MDO1 polytype and its twin-related MDO1' structure. This finding is in general agreement with the conclusion of Dornberger-Schiff & Höhne (1962), who suggested the occurrence of relatively coarse, ordered areas in the boulangerite crystals investigated by Berry (1940) and by Born & Hellner (1960). However, the OD groupoid symbol proposed by Dornberger-Schiff & Höhne (1962) was inadequate in explaining the space-group symmetry $Bb2_1m$ reported by Born & Hellner (1960). Instead, with the OD description developed in this work, we can fully describe all experimental evidence about boulangerite gathered so far.

X-ray single crystal and chemical data obtained from this work on the plumose boulangerite from Bottino reveal an almost ideal stoichiometry. The structural formula resulting from the refinement of the mono-clinic MDO1 polytype of boulangerite from Bottino is $Pb_{5.08}Sb_{3.93}S_{11}$, which is practically identical to the ideal formula $Pb_5Sb_4S_{11}$ of boulangerite and close to the formula $Pb_{4.89}(Sb_{4.08}As_{0.04}Bi_{0.01})_{\Sigma4.13}(S_{10.98}Se_{0.02})_{\Sigma11.00}$ resulting from electron-microprobe analyses (Table 1).

This chemical composition is in agreement (except for a different As content) with the average composition $Pb_{4.94}(Sb_{3.63}As_{0.43})_{\Sigma4.06}S_{11.00}$ determined by Orlandi et al. (2008) for boulangerite crystals coming from the same locality, but it is significantly different from that reported by Bechi (1852) and Garavelli (1957) on the same kind of material. In the latter cases, PbS/Sb$_2$S$_3$ values ranging from 2.05 to 2.26 were observed, which is significantly lower than the theoretical value, 2.5, expected for ideal boulangerite. Garavelli (1957) observed that a deficit of Pb is systematically present in boulangerite exhibiting a hairlike habit, whereas thicker crystals show an almost ideal composition. He thus concluded that the habit and density of boulangerite can be related to its composition. The deficit of Pb in hairlike boulangerite was explained by supposing the occurrence of vacancies in the structure according to the substitution $3Pb^{2+} \rightarrow 2Sb^{3+} + \square$. The possible existence of Pb-poor boulangerite according to the above substitution mechanism was postulated by Mumme (1989) as well. According to our structural model, we cannot exclude the possibility that vacancies may occur in the boulangerite framework, even though no evidence of their existence could be found from our study of plumose boulangerite from Bottino. Although our chemical data do show a minor increase of the trivalent (Sb+As+Bi) elements with respect to Pb, the resulting proportion of possible vacancies calculated from this substitution (~ 0.05 apfu) is too small to be considered reliable over the sum of cations.

Note that our electron-microprobe data, as well as those of Orlandi et al. (2008), do not confirm the deviation from the ideal stoichiometry of boulangerite reported by Garavelli (1957), although a similar material from the same deposit was the object of the

investigation. The reason may be related to differences in analytical techniques. The compositions described by Garavelli (1957) were in fact obtained by wet-chemical analyses, in which, as is well known, there can be significant errors related to the difficulties in obtaining homogeneous and pure material. Thus, it is possible that Garavelli (1957) may have had a small admixture of another fibrous sulfosalt in his material for wet-chemical analysis. Nevertheless, one cannot totally exclude the possible existence among natural material from Bottino of Pb-poor boulangerite. In this connection, we consider remarkable the find of some plumose crystals of boulangerite from the nearby Frigido mine, in the Apuan Alps, with a composition $(Pb_{4.17}Fe_{0.13}Cu_{0.09}Zn_{0.03}Ni_{0.03})_{\Sigma4.45}(Sb_{4.25}As_{0.04}Bi_{0.01})_{\Sigma4.30}S_{11}$ (PbS/Sb$_2$S$_3$ value: 2.07) reported by Carrozzini et al. (1993). However, the identification of these samples was based on results of electron-micro-probe analyses and X-ray powder diffraction investi-gations, and no single-crystal data could be obtained.

REFERENCES

Bechi, E. (1852): Intorno ad un nuovo minerale (meneghinite). Atti Accademia Georgofili 30, 84.

Bente, K. & Anton, R. (1995): Crystal chemistry and thin film epitaxy of sulphides and Bi-Sb-sulfosalts and their geological application. Mineral. Petrol. 53, 209-228.

Berlepsch, P., Makovicky, E. & Balić-Žunič, T. (2001a): Crystal chemistry of sartorite homologues and related sul-fosalts. Neues Jahrb. Mineral., Abh. 176, 45-66.

Berlepsch, P., Makovicky, E. & Balić-Žunič, T. (2001b): Crystal chemistry of meneghinite homologues and related sulfosalts. Neues Jahrb. Mineral., Monatsh., 115-135.

BERRY, L.G. (1940): Study of mineral sulpho-salts. III. Boulangerite and "epiboulangerite". *Univ. Toronto Studies, Geol. Ser.* **44**, 5-19.

BERRY, L.G. & THOMPSON, R.M. (1962): X-ray powder data for ore minerals: the Peacock atlas. *Geol. Soc. Am., Mem.* **85**.

BETTERIDGE, P.W., CARRUTHERS, J.R., COOPER, R.I., PROUT, K. & WATKIN, D.J. (2003): Crystals version 12: software for guided crystal structure analysis. *J. Appl. Crystallogr.* **36**, 1487.

BLESSING, R.H. (1995): An empirical correction for absorption anisotropy. *Acta Crystallogr.* **A51**, 33-38.

BORN, L. & HELLNER, E. (1960): A structural proposal for boulangerite. *Am. Mineral.* **45**, 1266-1271.

BOULANGER, C. (1835): Sur un sulfure double d'antimoine et de plomb de Molières, Département du Gard. *Ann. Mines* **7**, 575-582.

BRESE, N.E. & O'KEEFFE, M. (1991): Bond-valence parameters for solids. *Acta Crystallogr.* **B47**, 192-197.

BREITHAUPT, A. (1837): Embrithite, Plumbostib. *J. pr. Chem.* **10**, 442.

BRUKER (2003a): *APEX2*. Bruker AXS Inc., Madison, Wisconsin, USA.

BRUKER (2003b): *SAINT*. Bruker AXS Inc., Madison, Wisconsin, USA.

CARROZZINI, B., GARAVELLI, C.L. & VURRO, F. (1993): Zinkenite and associated sulfides and sulfosalts from the Frigido mine (Apuane Alps). *Per. Mineral.* **62**, 13-28.

COOK, N.J. & DAMIAN, G.S. (1997): New data on "plumosite" and other sulphosalt minerals from the Herja hydrothermal vein deposit, Baia Mare District, Rumania. *Geologica Carpathica* **48**, 387-399.

DITTRICH, H., BIENIOK, A, BRENDEL, U., GRODZICKI, M. & TOPA, D. (2007): Sulfosalts: a new class of compound semiconductors for photovoltaic applications. *Thin Solid Films* **515**, 5745-5750.

DORNBERGER-SCHIFF, K. (1956): On order–disorder structures (O–D structures). *Acta Crystallogr.* **9**, 593-601.

DORNBERGER-SCHIFF, K. (1964): Grundzüge einer Theorie von OD-Strukturen aus Schichten. *Abh. Dtsch. Akad. Wiss. Berlin. Kl. Chem. Geol. Biol.* **3**, 1-107.

DORNBERGER-SCHIFF, K. (1966): *Lehrgang über OD-Strukturen*. Akademie-Verlag, Berlin, Germany.

DORNBERGER-SCHIFF, K. & FICHTNER, K. (1972): On the symmetry of OD-structures consisting of equivalent layers. *Kristall und Technik* **7**, 1035-1056.

DORNBERGER-SCHIFF, K. & HÖHNE, E. (1962): Zur Symmetrie des Boulangerites. *Chem. Erde* **22**, 78-82.

ĎUROVIČ, S. (1997): Fundamentals of the OD theory. *In* Modular Aspects of Minerals (S. Merlino, ed.). *Eur. Mineral. Union, Notes in Mineralogy* **1**, 3-28.

FERRARIS, G., MAKOVICKY, E. & MERLINO, S. (2008): *Crystallography of Modular Materials*. IUCr/Oxford University Press, Oxford, U.K.

GARAVELLI, C.L. (1957): Contributo alla conoscenza della boulangerite. *Atti Soc. Tosc. Sci. Nat.* **64**, 133-151.

GUINIER, A., BOKIJ, G.B., BOLL-DORNBERGER, K., COWLEY, J.M., ĎUROVIČ, S., JAGODZINSKI, H., KRISHNA, P., DE WOLFF, P.M., ZVYAGIN, B.B., COX, D.E., GOODMAN, P., HAHN, T., KUCHITSU, K. & ABRAHAMS, S.C. (1984): Nomenclature of polytype structures. Report of the International Union of Crystallography *ad-hoc* Committee on the Nomenclature of Disordered, Modulated and Polytype Structures. *Acta Crystallogr.* **A40**, 399-404.

HAIDINGER, W. (1845): *Handbuch Der Bestimmenden Mineralogie*. Wien, Austria.

HEUER, M., WAGNER, G., DÖRING, T., BENTE, K. & KRYUKOVA, G. (2004): Nanowire arrangements of $PbS–Sb_2S_3$-compounds. *J. Crystal Growth* **267**, 745-750.

IBERS, J. A. & HAMILTON, W. C. (1974): *International Tables for X-ray Crystallography* **4**. The Kynoch Press, Birmingham, U.K.

JUMAS, J.C., OLIVIER-FOURCADE, J., PHILIPPOT, E. & MAURIN, M. (1980): Sur le système $SnS–Sb_2S_3$: étude structurale de $Sn_4Sb_6S_{13}$. *Acta Crystallogr.* **B36**, 2940-2945.

KRIVOVICHEV, S.V. (2008): Nanotubes in minerals and mineral-related systems. *In* Minerals as Advanced Materials I (S.V. Krivovichev, ed.). Springer, Heidelberg, Germany (179-191).

MAKOVICKY, E. (1981): The building principles and classification of bismuth–lead sulphosalts and related compounds. *Fortschr. Mineral.* **59**, 137-190.

MAKOVICKY, E. (1993): Rod-based sulphosalt structures derived from the SnS and PbS archetypes. *Eur. J. Mineral.* **5**, 545-591.

MAKOVICKY, E., BALIĆ-ŽUNIČ, T., KARANOVIĆ, L., POLETI, D. & PRČEK, J. (2004): Structure refinement of natural robinsonite, $Pb_4Sb_6S_{13}$: cation distribution and modular analysis. *Neues Jahrb. Mineral., Monatsh.*, 49-67.

MAKOVICKY, E. & HYDE, B.G. (1981): Non-commensurate (misfit) layer structures. *Struct. Bond.* **46**, 101-170.

MAKOVICKY, E. & MUMME, W.G. (1983): The crystal structure of ramdohrite, $Pb_6Sb_{11}Ag_3S_{24}$, and its implications for the andorite group and zinckenite. *Neues Jahrb. Mineral., Abh.* **147**, 58-79.

MAKOVICKY, E. & TOPA, D. (2009): The crystal structure of sulfosalts with the boxwork architecture and their new representative, $Pb_{15–2x}Sb_{14+2x}S_{36}O_x$. *Can. Mineral.* **47**, 3-24.

MAKOVICKY, E., TOPA, D. & MUMME, G.W. (2006): The crystal structure of dadsonite. *Can. Mineral.* **44**, 1499-1512.

MERLINO, S. (1997): OD approach in minerals: examples and applications. *In* Modular Aspects of Minerals (S. Merlino, ed.). *Eur. Mineral. Union, Notes in Mineralogy* **1**, 29-54.

MERLINO, S. (2009): OD approach to polytypism: examples, problems, indications. *Z. Kristallogr.* **224**, 251-260.

MOËLO, Y., MAKOVICKY, E., MOZGOVA N.N., JAMBOR, J.L., COOK, N. , PRING, A., PAAR, W., NICKEL, E.H., GRAESER, S., KARUP-MØLLER, S., BALIĆ-ŽUNIČ, T., MUMME, W.G., VURRO, F., TOPA, D., BINDI, L., BENTE, K. & SHIMIZU, M. (2008): Sulfosalt systematics: a review. Report of the sulfosalt sub-committee of the IMA Commission on Ore Mineralogy. *Eur. J. Mineral.* **20**, 7-46.

MOZGOVA, N.N. & BORTNIKOV, N.S. (1980): On non-stoichiometry of the acicular lead sulphantimonites. *In* Geochimiya – Mineralogiya. Nauka, Moscow, Russia (126-138).

MOZGOVA, N.N., BORTNIKOV, N.S., TSEPIN, A.I., BORODAEV, YU.S., VRUBLEVSKAJA, S.V., VYALSOV, L.N., KUZMINA, O.V. & SIVTSOV, A.V. (1983): Falkmanite, $Pb_{5.4}Sb_{3.6}S_{11}$, new data and relationship with sulphantimonites of lead (re-examination of type material from Bayerland mine, Bavaria). *Neues Jahrb. Mineral., Abh.* **147**, 80-98.

MUMME, W.G. (1989): The crystal structure of $Pb_{5.05}(Sb_{3.75}Bi_{0.28})S_{10.72}Se_{0.28}$: boulangerite of near ideal composition. *Neues Jahrb. Mineral., Monatsh.*, 498-512.

NESPOLO, M. & FERRARIS, G. (2001): Effects of the stacking faults on the calculated electron density of mica polytypes – the Ďurovič effect. *Eur. J. Mineral.* **13**, 1035-1045.

ORLANDI, P., MOËLO, Y. & BIAGIONI, C. (2008): Jamesonite delle miniere di Fornovolasco (Vergemoli, Lucca): primo ritrovamento sulle Alpi Apuane. *Atti Soc. tosc. Sci. nat., Mem.* **113**, 89-95.

PETROVA, I.V., KAPLUNNIK, L.N., BORTNIKOV, N.S., POBEDIMSKAYA, E.A. & BELOV, N.V. (1978b): Crystal structure of synthetic robinsonite. *Dokl. Akad. Nauk SSSR* **241**, 88-90 (in Russian).

PETROVA, I.V., KUZNETSOV, A.I., BELOKONEVA, E.L., SIMONOV, M.A., POBEDIMSKAYA, E.A. & BELOV, N.V. (1978a): Crystal structure of boulangerite. *Sov. Phys. Dokl.* **23**, 630-633.

PRUSETH, K.L., MISHRA, B. & BERNHARDT, H.-J. (2001): The minerals boulangerite, falkmanite and Cu-free meneghi-

nite: synthesis, new powder diffraction data and stability relations. *Eur. J. Mineral.* **13**, 411-419.

RAMDOHR, P. & ODMAN, O. (1940): Falkmanit, ein neues Bleispiessglanzerz, und sein Vorkommen, besonders in Boliden und Grube Bayerland. *Neues Jahrb. Mineral., Abt. A. Beih.* **75**, 315-350.

ROBINSON, S.C. (1948): The identity of falkmanite and yenerite with boulangerite. *Am. Mineral.* **33**, 716-723.

SHELDRICK, G.M. (1997): SHELXS–97: *A Program for Crystal Structure Refinement*. University of Göttingen, Göttingen, Germany.

SHELDRICK, G.M. (2008): SADABS: *Program for Empirical Absorption Correction of Area Detector Data*. University of Göttingen, Göttingen, Germany.

SKOWRON, A. & BROWN, I.D. (1990a): Refinement of the structure of boulangerite, $Pb_5Sb_4S_{11}$. *Acta Crystallogr.* **C46**, 531-534.

SKOWRON, A. & BROWN, I.D. (1990b): Refinement of the structure of robinsonite, $Pb_4Sb_6S_{13}$. *Acta Crystallogr.* **C46**, 527-531.

SMITH, P.P.K. & HYDE, B.G. (1983): The homologous series $Sb_2S_3 \bullet nPbS$: structures of diantimony dilead pentasulphide, $Pb_2Sb_2S_5$, and the related phase diantimony ditin pentasulphide, $Sn_2Sb_2S_5$. *Acta Crystallogr.* **C39**, 1498-1502.

STASI, F., VURRO, F. & RENNA, M. (1998): Boulangerite from Bottino mine (Apuane Alps): twinning and OD character. Proc. 78th Convegno SIMP (Monopoli). *Plinius* **20**(2), 201-203.

ŠTRBAC, N., MIHAJLOVIČ, I., MINIĆ, D. & ŽIVKOVIĆ, Ž. (2010): Characterization of the natural mineral form from the PbS–Sb_2S_3 system. *J. Mining Metall., Sect. B Metall.* **46**, 75-86.

THAULOW, M.C.J. (1837): Analyse eines Antimonerzes vom Nasafjeld in Lapland. *Annalen der Physik und Chemie* **41**, 216-221.

WANG, N. (1973): A study of the phases on the pseudobinary join PbS–Sb_2S_3. *Neues Jahrb. Mineral., Monatsh.*, 79-81.

WANG, N. (1977): Synthesis and crystal data on a Cu-free "meneghinite". *Can. Mineral.* **15**, 115-116.